Advances in Materials Research, *Vol. 13, No. 3 (2024) 153-160*
https://doi.org/10.12989/amr.2024.13.3.153

AC and DC anodization on the electrochemical properties of SS304L: A comparison

Nur S. Azmi[1], Mohd N. Derman*[1,2] and Zuraidawani Che Daud[1,2a]

[1]*Faculty of Mechanical Engineering and Technology, Universiti Malaysia Perlis (UniMAP), Kampus Tetap Pauh Putra, 02600 Arau, Perlis, Malaysia*
[2]*Frontier Materials Research, Centre of Excellence (FrontMate), Universiti Malaysia Perlis (UniMAP), Kampus Tetap Pauh Putra, 02600 Arau, Perlis, Malaysia*

(*Received July 28, 2023, Revised September 18, 2023, Accepted January 5, 2024*)

Abstract. This study investigates the application of alternating current (AC) and direct current (DC) anodization techniques on stainless steel 304L (SS304L) in an ethylene glycol and ammonium fluoride (NH4F) electrolyte solution to produce a nano-porous oxide layer. With limited research on AC anodizing of stainless steel, this study focuses on comparing AC and DC anodization in terms of current density versus time response, phase analysis using X-ray diffraction (XRD), and corrosion rate determined by linear polarization. Both AC and DC anodization were performed for 60 minutes at 50 V in an electrolyte solution containing 0.5% NH4F and 3% H_2O in ethylene glycol. The results show that AC anodization exhibited higher current density compared to DC anodization. XRD analysis revealed the presence of ferrite (α-Fe) and austenite (γ-Fe) phases in the as-received specimen, while both AC and DC anodized specimens exhibited only the γ-Fe phase. The corrosion rate of the AC-anodized specimen was measured at 0.00083 mm/year, lower than the corrosion rate of the DC-anodized specimen at 0.00197 mm/year. These findings indicate that AC anodization on stainless steel offers advantages in terms of higher current density, phase transformation, and lower corrosion rate compared to DC anodization. These results highlight the need for further investigation and exploration of AC anodization as a promising technique for enhancing the electrochemical properties of stainless steel.

Keywords: AC anodizing; corrosion rate; DC anodizing; linear polarization; stainless steel 304L

1. Introduction

Nanomaterials had gained attention due to their outstanding characteristics and ability to form nano-porous structures at the nanoscale. Materials with nano-porous structures have made significant improvement in areas such as energy conversion and storage, sensing, and biological applications (Hassan *et al.* 2020). Anodizing is one among the various techniques used to form nano-porous materials that offers good control over pore size, shape, and distribution. Large numbers of anodizing studies had focused on aluminum (Al) and its alloys with countless studies focused on understanding the generation and behavior of nano-porous oxide film on their surfaces (Pawlik *et*

*Corresponding author, Associate Professor, E-mail: nazree@unimap.edu.my
[a]Ph.D., E-mail: zuraidawani@unimap.edu.my

http://www.techno-press.org/?journal=amr&subpage=5 ISSN: 2234-0912 (Print), 2234-179X (Online)

al. 2017).

However, in early 2000's the anodization of stainless steel had grown in interest because of its high mechanical qualities and corrosion resistance (Naresh and Rajasekhar 2016). The stainless steel is a versatile material that could be utilized extensively in a variety of fields (Wang *et al.* 2019). It is possible to modify the surface characteristics of stainless steel and improve its performance in particular uses by anodizing it. Comparing to other materials, the works related to stainless steel anodization involves some distinct issues. Stainless steel is an alloy mainly composed of iron (Fe) with various proportions of chromium (Cr), nickel (Ni), and other metals. Stainless steel is classified into three primary types: austenitic, ferritic, and martensitic (Banerjee 2015). Among these, austenitic stainless steel, particularly Type 304L, is widely utilized due to its excellent properties, with the "L" signifying its extra-low carbon content (Singh *et al.* 2018).

Anodizing, a widely employed technique, enables the synthesis of nano-porous oxide films on alloy surfaces. While anodizing of alloys such as Al, Mg, and Ti is well-known, its application to stainless steel has been an area of growing research (Pawlik *et al.* 2017). Pioneered by Grimes and colleagues, anodizing techniques have been utilized to produce nano-porous oxide films on iron substrates in ethylene glycol solutions containing NH_4F and H_2O (Jagminas *et al.* 2011). Various factors influence the formation of nano-porous oxide films, including the applied current or voltage, type and concentration of the electrolyte, electrolyte temperature, and anodization time (Sulka 2020). The most popular anodizing method is two-step anodizing involves a chemical etching process before the anodization step, although this can lead to chemical corrosion and liquid pollution (Wu *et al.* 2019).

Conventionally, direct current (DC) has been widely used as the power source for anodization due to its simplicity and ease of control. There have been few studies on AC anodizing and the studies are focusing on alloys such as aluminum and titanium. As a result, the purpose of this research is to analyze and evaluate the effects of AC and DC anodizing on current density versus time response, phase analysis, and corrosion rate on stainless steel 304L. A thorough comparison investigation can provide useful insights into the electrochemical characteristics of AC- and DC-anodized stainless steel, leading the way for further developments in stainless steel anodization processes.

2. Materials and methods

2.1 Material and chemical preparation

The stainless steel 304L (SS304L) material was used as the raw material for this study, with its composition specified in Table 1 (Patricia *et al.* 2022). Rectangular specimens measuring 25 mm×15 mm×2 mm were prepared by cutting the SS304L plates. The specimens underwent a series of preparation steps, including grinding up to 1200-grit paper and polishing with diamond paste to achieve a mirror-like surface finish. Electroplating tape was applied to ensure exposure is controlled. So that only one surface of the specimens is exposed. Prior to anodization, the specimens were degreased using acetone and thoroughly rinsed with distilled water.

2.2 Anodization process

The anodization experiments were conducted using a basic setup equipped with AC or DC power

Table 1 The chemical composition of SS304L (wt%)

Fe	Cr	Ni	Mn	Si	C	P	S
Balance	18.0-20.0	8.0-12.0	≤2.0	≤0.75	≤0.03	≤0.045	≤0.03

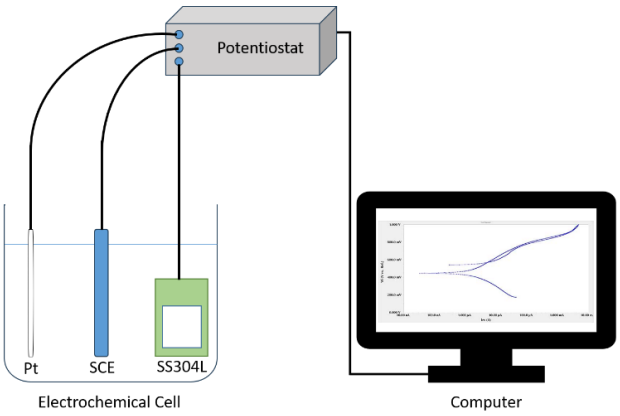

Fig. 1 The three-electrode cell setup for polarization test

sources in 250 mL beaker. Two SS304L electrodes were employed in the anodization process. Anodization was carried out for 60 minutes at room temperature, applying an anodizing voltage of 50 V for both AC and DC power sources. The primary focus of this study was to investigate the differences between AC and DC anodization. During the anodization process, the anodizing current was recorded as an output parameter, and the current density was subsequently calculated. Following anodization, the specimens were meticulously rinsed with distilled water and dried using an air dryer.

2.3 XRD analysis

Phase analysis of the specimens before and after anodization was performed using a Shimadzu XRD 6000 diffractometer. The XRD measurements covered 2θ values ranging from 20° to 80°, employing Cu Kα radiation. Each step of the measurement had a fixed counting time of 0.3 seconds. The obtained XRD data were analyzed using the X'Pert HighScore Plus software to determine the phases present.

2.3 Linear polarization

The linear polarization test utilized an AUTOLAB PGSTAT 204 potentiostat and NOVA software. A three-electrode corrosion cell system was employed, consisting of the specimen as the working electrode, a saturated calomel electrode (SCE) as the reference electrode, and a platinum rod as the counter electrode as shown in Fig. 1. To ensure a consistent exposed area, the specimen's surface was covered with electroplating tape, leaving only a 1 cm^2 region exposed. Open-circuit potential (OCP) measurements were conducted over 30 minutes to achieve a stable state. OCP represents the potential of the working electrode relative to the reference electrode when no potential or current is applied to the corrosion system. This measurement is vital for predicting the electrochemical corrosion behavior of the specimens in the test medium. The polarization scans were

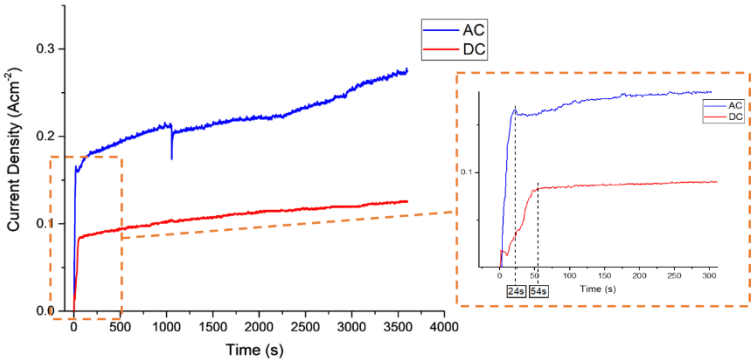

Fig. 2 Current-time responses for 1 hour anodizing of SS304L in ethylene glycol solution containing NH_4F and H_2O

performed at a scanning rate of 10 mVs^{-1}, covering a scan potential range from -0.8 V to 1.0 V versus SCE.

3. Result and discussions

3.1 Current density versus time response

For the study of the differences between AC and DC methods in forming the nano-porous oxide layer on SS304L, it is essential to analyze the current density versus time responses during anodization. In Fig. 2, the current density versus time responses for AC and DC anodization of SS304L at 50 V for 60 minutes are presented. Notably, AC anodization resulted in a higher current density than DC, emphasizing the differences between both power sources. Both methods showed a similar general trend, with the current growing fast and then plateauing. The observed stability of the DC anodization current density suggests a controlled and consistent anodization process, which may influence the uniformity and quality of the nano-porous oxide layer. AC anodization, on the other hand, continued to show a rising trend with increased anodization duration, indicating a periodic reversal of electric charge flow (Li *et al.* 2013). The current density of the AC specimen reached from 0 Acm^{-2} to 0.165 Acm^{-2} in 24 seconds, whereas the DC specimen increased more gradually, reaching 0.084 Acm^{-2} in 54 seconds.

3.2 XRD analysis

The XRD pattern analysis of the as-received SS304L specimen, as well as the AC and DC anodized SS304L specimens, is shown in Fig. 3. The as-received specimen exhibited the presence of austenite (γ-Fe) peaks at 43.7°, 50.9°, and 74.9°, along with ferrite (α-Fe) peak at 44.7°. The presence α-Fe peak can be attributed to the mechanical polishing step performed before anodization, which aligns with previous findings (Rao *et al.* 2005). Interestingly, the XRD patterns of the as-received and anodized specimens using both AC and DC sources exhibited similarities, indicating the absence of distinct oxide layer peaks. This can be attributed to the amorphous or poorly crystalline nature of the nano-porous oxide layer formed during anodization (Saha *et al.* 2019).

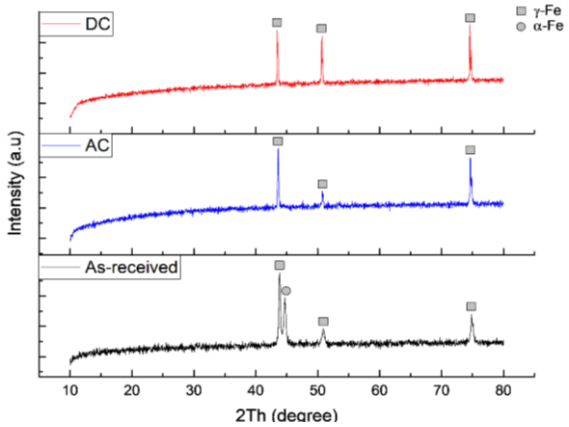

Fig. 3 XRD pattern of as-received stainless steel and anodized stainless steel using AC and DC power source

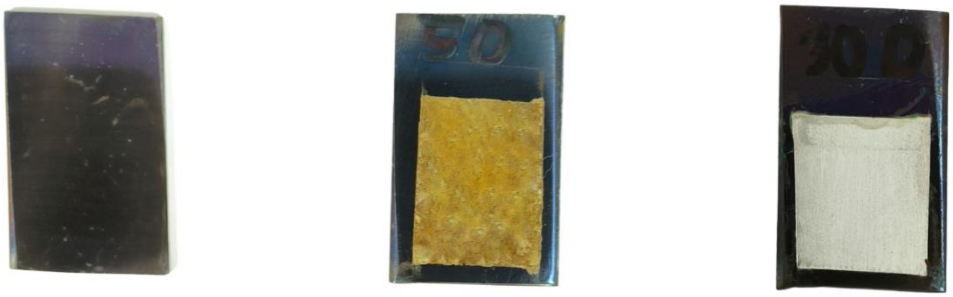

(a) As-received specimen (b) AC-anodized specimen (c) DC-anodized specimen

Fig. 4 The specimens of (a) As-received and after anodizing process using, (b) AC and (c) DC sources

Previous studies by Saha et al. demonstrated that the detection of the Fe_2O_4 oxide layer only occurred after thermal treatment, while the nano-porous oxide layer was visible without distinct peaks. Moreover, the observed color variations between AC and DC specimens as shown in Fig. 4, with AC showing a yellowish layer and DC displaying a greyish layer, further demonstrate the diverse nature of the oxide layers formed under different anodization conditions. Notably, Klimas *et al.*'s findings of color changes during anodization at varying voltages add weight to our observations (Klimas *et al.* 2013).

3.3 Linear polarization

The findings of the linear polarization test performed on specimens immersed in a 3.5% NaCl solution are shown in Table 2. The corrosion potential (E_{corr}) and corrosion current (I_{corr}) were determined by extrapolating the polarization curve depicted in Fig. 5 while the corrosion rate was extracted from the NOVA software. However, equation (1) could also be use in order to obtain the corrosion rate of the SS304L. E_{corr} serves as an indicator of the likelihood of corrosion during the test, while I_{corr} quantifies the severity of corrosion experienced by the specimens (Heo *et al.* 2021).

Table 2 Result of linear polarization for as-received, AC and DC anodized specimens

Specimens	E_{corr} (V)	I_{corr} (A/cm^2)	Corrosion Rate (mm/year)
As-received	-0.2832	7.380×10-7	0.00857
DC	-0.2398	1.696×10-7	0.00197
AC	0.04489	7.140×10-8	0.00083

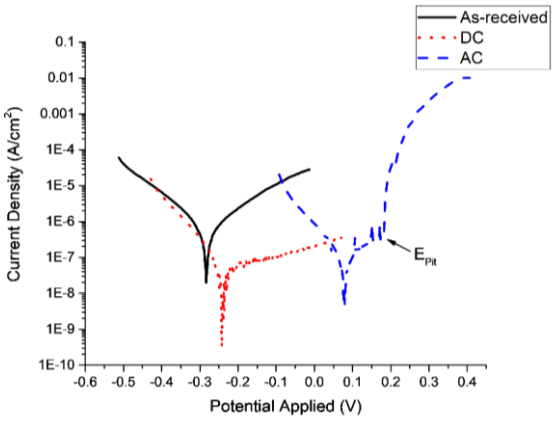

Fig. 5 The polarization curve of as-received, AC and DC anodized specimens

The E_{corr} value of the as-received specimen, which had no protective coating, was -0.2832 V. Notably, both the DC and AC anodized specimens demonstrated a shift towards more positive E_{corr} values, measuring -0.2398 V and 0.04489 V, respectively. This change from more negative to more positive potentials suggests improved corrosion resistance for both DC and AC specimens (Jamil *et al.* 2018, Saha *et al.* 2019). Specifically, the AC-anodized specimens corroded at a substantially lower rate of 0.00083 mm/year than DC-anodized specimens, which corroded at a rate of 0.00197 mm/year. This difference in corrosion rates was due to the unique characteristics of the oxide layer generated during AC anodization. The nano-porous oxide layer formed by AC anodizing appears to provide greater corrosion protection, resulting in a decreased corrosion rate reported when compared to DC-anodized specimens.

$$Corrosion\ Rate\ (mm/year) = 3.27 \times I_{corr} \times \frac{EW}{d} \quad (1)$$

Where, EW is equivalent weight of SS304L, which is 25.12 and d is the density of SS304L, which is 7.93 gcm^{-3}. The Icorr is also converted into unit of mAcm^{-2}.

The data in Fig. 5 clearly illustrated the corrosion behavior of the specimens, where both DC and AC specimens exhibited a movement towards more positive E_{corr} values in comparison to the as-received specimen. This shift indicated the formation of a protective nano-porous oxide layer on the surface of the specimen, which contributes to improved corrosion resistance (Hernández López *et al.* 2019). Furthermore, the polarization curve of the AC specimen reveals the presence of a distinct pitting potential, E_{pit}, as labeled in Fig 5. E_{pit} represents the potential at which the breakdown of the passive layer occurs, leading to localized corrosion in the form of pits.

These findings indicated that both DC and AC anodization contribute to improved corrosion resistance, with the AC-anodized specimens demonstrating the highest resistance owing to the

presence of a nano-porous oxide layer. The observed pitting potential in the AC specimen suggests that the anodized surface may exhibit localized corrosion susceptibility under specific conditions, requiring further investigation.

4. Conclusions

In conclusion:

• The current density versus time graph analysis demonstrated that AC anodizing resulted in a larger current density than DC anodizing.

• AC current density achieved a plateau after 24 seconds, but DC current density took 54 seconds to stabilize.

• XRD examination of the specimens revealed the presence of γ-Fe and α-Fe in the as-received specimen, but only γ-Fe peaks in the AC and DC specimens, indicating the creation of an amorphous oxide layer.

• In terms of corrosion rate, the AC specimen displayed the lowest rate at 0.00083 mm/year, while the DC specimen exhibited a corrosion rate of 0.00197 mm/year. Notably, both AC and DC anodized specimens demonstrated lower corrosion rates compared to the as-received specimen, which exhibited a corrosion rate of 0.00857 mm/year. These results highlight the potential benefits of AC anodizing for enhancing the electrochemical and corrosion properties of SS304L.

Acknowledgments

The author would like to acknowledge the support from the Fundamental Research Grant Scheme (FRGS) under the grant number FRGS/1/2019/TK10/UNIMAP/02/2 from the Ministry of Higher Education Malaysia. Special thanks to Centre of Excellence for Frontier Materials Research (FrontMate) and Institute of Nano Electronic Engineering (INEE) for providing facilities and testing this project.

References

Banerjee, M.K. (2015), "Microstructural engineering of dual phase steel to aid in bake hardening", *Adv. Mater. Res.*, **4**(1), 1-12. https://doi.org/10.12989/amr.2015.4.1.1.

Hassan, A., Ali, G., Park, Y.J., Hussain, A. and Cho, S.O. (2020), "Formation of a self-organized nanoporous structure with open-top morphology on 304L austenitic stainless steel", *Nanotechnol.*, **31**(31), 315603. https://doi.org/10.1088/1361-6528/ab8997.

Heo, J., Lee, S.Y., Lee, J., Alfantazi, A. and Cho, S.O. (2021), "Improvement of corrosion resistance of stainless steel welded joint using a nanostructured oxide layer", *Nanomater.*, **11**(4), 1-13. https://doi.org/10.3390/nano11040838.

Hernández López, J.M., Dominguez Jaimes, L.P., Alvarez mendez, A., Sanchez Vazquez, A., Ruiz Valdes, J.J., Cedillo González, E.I., Conde del Campo, A., De Damborenea González, J.J., Arenas Vara, M.A., Patricia, L., Jaimes, D., Álvarez Méndez, A., Sánchez Vázquez, A., Jacobo, J., Valdés, R., Cedillo González, E.I., Conde del Campo, A., De Damborenea González, J.J., Ángeles, M. and Manuel Hernández López, J. (2019), "Corrosion resistance of anodic layers grown on 304L stainless steel at different anodizing

times and stirring speeds", *Proceedings of the 1st Coatings and Interfaces Web Conference*, Basel, Switzerland, March.

Jagminas, A., Klimas, V., Mažeika, K., Bernotas, N., Selskis, A. and Niaura, G. (2011), "Fabrication of thick gel-like films by anodizing iron in a novel electrolyte based on dimethyl sulfoxide and H_2SiF_6", *Electrochim. Acta*, **56**(16), 5452-5458. https://doi.org/10.1016/j.electacta.2011.03.011.

Jamil, A.A., Derman, N. and Azmi, S. (2018), "Comparison study of magnesium anodizing by using alternating current (AC) and direct current (DC)", *Int. J. Current Res. Sci. Eng. Tech.*, **1**(Spl-1), 307. https://doi.org/10.30967/ijcrset.1.S1.2018.307-312.

Klimas, V., Pakštas, V., Vrublevsky, I., Chernyakova, K. and Jagminas, A. (2013), "Fabrication and characterization of anodic films onto the type-304 stainless steel in glycerol electrolyte", *J. Phys. Chem. C*, **117**(40), 20730-20737. https://doi.org/10.1021/jp407028u.

Li, W., Li, W., Zhu, L., Liu, H. and Wang, X. (2013), "Non-sparking anodization process of AZ91D magnesium alloy under low AC voltage", *Mater. Sci. Eng.: B*, **178**(7), 417-424. https://doi.org/10.1016/j.mseb.2013.01.008.

Naresh, N. and Rajasekhar, K. (2016), "Multi-response optimization for milling AISI 304 Stainless steel using GRA and DFA", *Adv. Mater. Res.*, **5**(2), 67-80. https://doi.org/10.12989/amr.2016.5.2.067.

Patricia, L., Arenas, A., Conde, A., Escobar-morales, B., Anabel, Á. and Manuel, J. (2022), "Growth of anodic layers on 304L stainless steel using fluoride free electrolytes and their electrochemical behavior in chloride solution", *Mater.*, **15**(5), 1892. https://doi.org/10.3390/ma15051892.

Pawlik, A., Hnida, K., Socha, R.P., Wiercigroch, E., Małek, K. and Sulka, G.D. (2017), "Effects of anodizing conditions and annealing temperature on the morphology and crystalline structure of anodic oxide layers grown on iron", *Appl. Surf. Sci.*, **426**, 1084-1093. https://doi.org/10.1016/j.apsusc.2017.07.156.

Rao, K.R.M., Mukherjee, S., Raole, P.M. and Manna, I. (2005), "Characterization of surface microstructure and properties of low-energy high-dose plasma immersion ion-implanted 304L austenitic stainless steel", *Surf. Coat. Technol.*, **200**(7), 2049-2057. https://doi.org/10.1016/j.surfcoat.2004.06.035.

Saha, S.K., Park, Y.J., Kim, J.W. and Cho, S.O. (2019), "Self-organized honeycomb-like nanoporous oxide layer for corrosion protection of type 304 stainless steel in an artificial seawater medium", *J. Molecular Liqs.*, **296**, 111823. https://doi.org/10.1016/j.molliq.2019.111823.

Singh, R., Sachan, D., Verma, R., Goel, S., Jayaganthan, R. and Kumar, A. (2018), "Mechanical behavior of 304 Austenitic stainless steel processed by cryogenic rolling", *Mater. Today: Proc.*, **5**(9), 16880-16886. https://doi.org/10.1016/j.matpr.2018.04.090.

Sulka, G.D. (2020), "Introduction to anodization of metals", *Nanostructured Anodic Metal Oxides*, Elsevier, Amsterdam, Netherlands.

Wang, Y., Li, G., Wang, K. and Chen, X. (2019), "Fabrication of thick anodic films on 304-type stainless steel for binder-free supercapacitors", *11th International Conference on Nanomaterials - Research & Application*, Brno, Czech Republic, October.

Wu, Y., Zhao, F., Zhang, Z. and Li, L. (2019), "Study on the preparation and properties of micro-nano structure on the surface of 304 stainless steel by one-step anodizing", *J. Nano Res.*, **60**, 42-50. https://doi.org/10.4028/www.scientific.net/JNanoR.60.42.